

Metrology of Wide-Viewing-Angle $\lambda/4$ Plate in lithography

Juan Dong^a, Peng Du^b

Dept. of engineering physics, School of Tsinghua University, Beijing 100084, China;
^adongjuan@tsinghua.edu.cn

Keywords: Metrology; waveplate; wide viewing angle; phase; retardation; oblique incidence

Abstract. Waveplates are among the most commonly used devices for altering the polarization state of light, and have been widely applied in polarization analysis of high-numerical-aperture (high-NA) imaging systems such as polarizing microscopes and immersion lithographers. As the NA of an optical system is increased, the effects of oblique incidence on the phase retardation of light rays passing through a waveplate become increasingly significant. This paper describes the design and manufacture of a 632.8 nm wide-viewing-angle (WVA) $\lambda/4$ plate. The method of phase compensation is employed to measure the phase retardation characteristics of this waveplate. These experimental results show that the phase retardation by the WVA $\lambda/4$ plate is consistently in the range between 84° and 96° for angles of incidence between $\pm 20^\circ$, which confirms the effectiveness of the combination of positive and negative crystal in eliminating the influence of oblique incidence on phase retardation.

INTRODUCTION

As the feature size of integrated circuits shrinks, there is an increasing demand for high resolution in high-numerical-aperture (high-NA) optical imaging.^{1,2} However, the quality and resolution of such high-NA imaging systems are susceptible to the effects of polarization. Accordingly, the effect of oblique incidence of a light ray on its phase retardation by a waveplate—one of the key components of a polarimeter—has become a topic of great interest.

In the polarimetry of a high-NA lithographer, measurements of the state of polarization of light and the polarization aberration of projection optics at the mask level are affected by the precision of the wide-viewing-angle (WVA) $\lambda/4$ plate. Consequently, a suitable method of measurement that ensures accurately gauged retardation is a prerequisite for minimizing errors induced by a waveplate, and therefore significant for its utilization in high-precision measurement.

There are a variety of techniques for measuring retardation by a waveplate, including polarization-interference,^{3–7} phase-modulation,^{8,9} optical heterodyning,^{10,11} phase-shifting,^{12,13} and phase compensation,^{14–17} among others. Phase compensation is one of the most commonly used, owing to the relatively low complexity of the light path and its ease of adjustment, as well as the high precision of the results.

PRINCIPLES OF PHASE COMPENSATION

The principle of phase compensation, also known as de Sénarmont compensation, is illustrated in Figure 1. The system consists of a polarizer, the waveplate to be measured, a standard $\lambda/4$ plate, and a polarization analyzer. The retardation by the target waveplate can be determined based on the variation in light intensity as the polarization analyzer is rotated while the first three devices are held fixed.

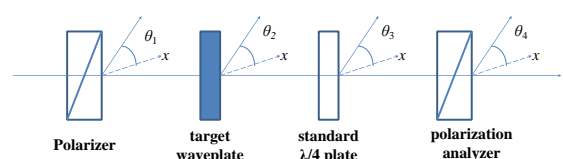


Fig.1 Measurement of waveplate retardation using the phase compensation method

The direction of propagation of the incident ray is taken as the z axis, and the azimuthal angles of the polarizer, target waveplate, standard $\lambda/4$ plate, and polarization analyzer are denoted by θ_1 , θ_2 ,

θ_3 , and θ_4 , respectively. The Mueller matrices of the four devices are denoted by P_1 , Q_2 , Q_3 , and P_4 , respectively, and are represented as follows:

$$P_1 = \frac{1}{2} \begin{pmatrix} 1 & \cos 2\theta_1 & \sin 2\theta_1 & 0 \\ \cos 2\theta_1 & \cos^2 2\theta_1 & \cos 2\theta_1 \sin 2\theta_1 & 0 \\ \sin 2\theta_1 & \cos 2\theta_1 \sin 2\theta_1 & \sin^2 2\theta_1 & 0 \\ 0 & 0 & 0 & 0 \end{pmatrix}$$

$$Q_2 = \begin{pmatrix} 1 & 0 & 0 & 0 \\ 0 & \cos^2 2\theta_2 + \cos \delta \sin^2 2\theta_2 & (1 - \cos \delta) \sin 2\theta_2 \cos 2\theta_2 & -\sin \delta \sin 2\theta_2 \\ 0 & (1 - \cos \delta) \sin 2\theta_2 \cos 2\theta_2 & \sin^2 2\theta_2 + \cos \delta \cos^2 2\theta_2 & \sin \delta \cos 2\theta_2 \\ 0 & \sin \delta \sin 2\theta_2 & -\sin \delta \cos 2\theta_2 & \cos \delta \end{pmatrix}$$

$$Q_3 = \begin{pmatrix} 1 & 0 & 0 & 0 \\ 0 & \cos^2 2\theta_3 & \sin 2\theta_3 \cos 2\theta_3 & -\sin 2\theta_3 \\ 0 & \sin 2\theta_3 \cos 2\theta_3 & \sin^2 2\theta_3 & \cos 2\theta_3 \\ 0 & \sin 2\theta_3 & -\cos 2\theta_3 & 0 \end{pmatrix}$$

$$P_4 = \frac{1}{2} \begin{pmatrix} 1 & \cos 2\theta_4 & \sin 2\theta_4 & 0 \\ \cos 2\theta_4 & \cos^2 2\theta_4 & \cos 2\theta_4 \sin 2\theta_4 & 0 \\ \sin 2\theta_4 & \cos 2\theta_4 \sin 2\theta_4 & \sin^2 2\theta_4 & 0 \\ 0 & 0 & 0 & 0 \end{pmatrix},$$

where δ is the retardation of the measured waveplate. The Stokes parameters of the emergent ray can then be represented as

$$\begin{bmatrix} s'_0 & s'_1 & s'_2 & s'_3 \end{bmatrix}^T = P_4 \cdot Q_3 \cdot Q_2 \cdot P_1 \cdot \begin{bmatrix} s_0 & s_1 & s_2 & s_3 \end{bmatrix}^T. \quad (1)$$

Substituting P_1 , Q_2 , Q_3 , and P_4 into (1), the intensity of the incident ray can be derived as

$$I = s'_0 = \frac{s_0 + \cos 2\theta_1 \cdot s_1 + \sin 2\theta_1 \cdot s_2}{4} \cdot \{1 + \cos(2\theta_4 - 2\theta_3)(1 - \cos \delta) \cos(2\theta_3 - 2\theta_2) \cos(2\theta_2 - 2\theta_1) + \cos(2\theta_4 - 2\theta_3) \cos \delta \cos(2\theta_3 - 2\theta_1) + \sin(2\theta_4 - 2\theta_3) \sin \delta \sin(2\theta_2 - 2\theta_1)\}. \quad (2)$$

By the principle of phase compensation, the relationships between the azimuthal angles of the four devices are as follows:

$$\begin{aligned} \theta_2 &= \theta_1 + 45^\circ \\ \theta_3 &= \theta_1 \\ \theta_4 &= \theta_0 + \theta \\ \theta_0 &= \theta_1 + 90^\circ \end{aligned} \quad (3)$$

where θ_0 and θ are the initial azimuthal angle and the rotation angle, respectively, of the polarizer P_4 . Substitution of (3) into (2) gives

$$I = 1 - \cos(\delta - 2\theta). \quad (4)$$

It can be seen from (4) that, with the phase compensation method, the retardation δ by the target waveplate is given by twice the angle θ through which the polarization analyzer has to be rotated to make the field of view darkest:

$$\delta = 2\theta. \quad (5)$$

The detailed measurement procedure is as follows:

1. Rotate the polarization analyzer P_4 while keeping the transmission direction of the polarizer P_1 fixed until the system output becomes zero. Then place the standard $\lambda/4$ plate Q_3 between P_1 and P_4 , before rotating it to align its optical direction with the transmission direction of P_1 when the field of view is darkest.
2. Place the target waveplate Q_2 between the polarizer P_1 and the standard $\lambda/4$ plate Q_3 , and rotate it until the field of view is darkest, which indicates that the optical direction of Q_2 is parallel to the transmission direction of P_1 . Then continue the rotation until the angle between the optical direction of Q_2 and the transmission direction of P_1 is 45° . A relatively bright field of view is present, but not at the maximum level. If the target waveplate is a standard $\lambda/4$ plate, the brightness is approximately one-half of the maximum.
3. Rotate the polarization analyzer P_4 and note the angle of rotation when the field of view is darkest. The retardation by the target waveplate can then be calculated using (5). By definition, clockwise rotation produces negative values of the angle, while anticlockwise rotation produces positive values.

EXPERIMENTAL SYSTEM

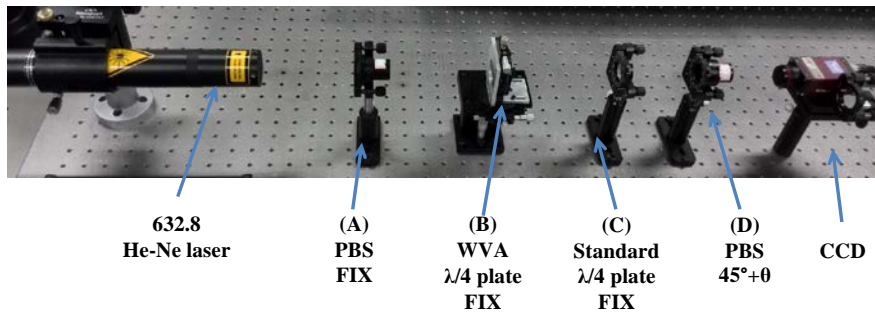


Fig.2 Group of devices for measuring retardation by a WVA $\lambda/4$ plate

The group of optical devices for measuring retardation by a WVA $\lambda/4$ plate shown in Figure 2 consists of a polarized beam splitter (PBS) A (the polarizer), a WVA $\lambda/4$ plate B composed of two pieces of sapphire and two pieces of crystal quartz (the target waveplate), a standard $\lambda/4$ plate C, a polarized beam splitter D (the polarization analyzer), and an opto-electronic detector. The combinations of the azimuthal angles of A, C, and D based on three different states of the incident plane on B during the measurement process described in Section 1 are shown in Table 1.

Table 1 Azimuthal angles of the four devices

PBS (A)	WVA $\lambda/4$ plate (B)	Standard $\lambda/4$ plate (C)	PBS (D)
-45°	0°	-45°	$45^\circ + \theta$
0°	45°	0°	$90^\circ + \theta$
45°	90°	45°	$-45^\circ + \theta$

The incident and azimuthal angles of the incident plane on B are illustrated in Figure 3.

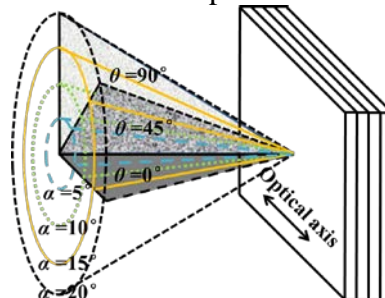


Fig.3 Obliquely incident ray on the WVA $\lambda/4$ plate characterized by the incident angle and azimuthal angle of the incident plane

This group of devices is illuminated by a He–Ne laser operating at a wavelength of 632.8 nm and producing a linearly polarized light beam along the x direction. The purity of polarization of the devices is defined as

$$P_p = \frac{I_{\max} - I_{\min}}{I_{\max} + I_{\min}},$$

where I_{\max} and I_{\min} are the transmittances of the optical components propagating along and perpendicular to the optical axis, respectively. The minimum degree of polarization of the He–Ne laser is 99.8%. The polarized beam splitter A is able to produce linearly polarized light of high purity along any direction. The detector measures the intensity of the incident ray as its angle of incidence α turns from -20° to 20° at intervals of 5° . An example is shown in Figure 4, where the incident ray on the WVA $\lambda/4$ plate is inside the plane of incidence with a 45° azimuthal angle. The figure shows that the light output of the detector is lowest when D rotates into zones close to -45° , for every incident ray on the WVA $\lambda/4$ plate. The retardation by the target waveplate varies with incident angle, and its characteristic curve can be obtained by least squares fitting of the measurement data.

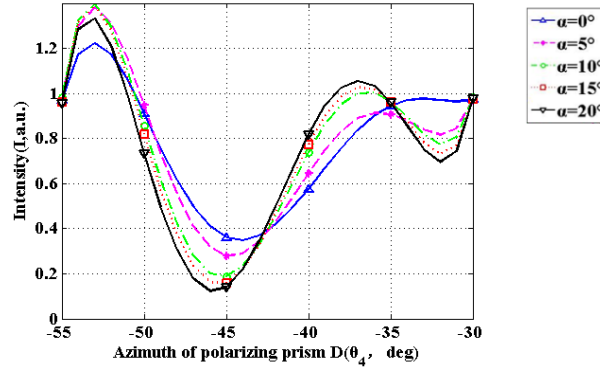


Fig.4 Relationship between measured intensity and azimuthal angle of the polarized beam splitter D as the incident angle α turns from -20° to $+20^\circ$ for an azimuthal angle of the incident plane $\theta_2=45^\circ$

RESULTS AND DISCUSSION

A conventional double-plate-type $\lambda/4$ plate is only able to produce phase retardation of 90° at normal incidence. In contrast, a four-plate WVA $\lambda/4$ plate can produce phase retardation of 90° at normal incidence, as well as a value close to this ($90^\circ \pm 0.5^\circ$, Table 2) at a high NA of 1.35, which is equivalent to an incident angle of $\pm 20^\circ$ at the mask level. This result is obtained by substituting the design values of the thicknesses of the four crystal pieces ($d_1=584.2 \mu\text{m}$, $d_2=566.6 \mu\text{m}$, $d_3=848.4 \mu\text{m}$, and $d_4=848.4 \mu\text{m}$) into the WVA $\lambda/4$ plate retardation equation(13) in reference 18, i.e.

$$\begin{aligned} \delta &= \delta_1 + \delta_2 \\ &= \frac{2\pi d_1}{\lambda} \left(\sqrt{n_e^2 - \frac{n_e^2 \cos^2 \theta + n_o^2 \sin^2 \theta}{n_o^2} \sin^2 \alpha} - \sqrt{n_o^2 - \sin^2 \alpha} \right) \\ &+ \frac{2\pi d_2}{\lambda} \left(\sqrt{n_o^2 - \sin^2 \alpha} - \sqrt{n_e^2 - \frac{n_e^2 \sin^2 \theta + n_o^2 \cos^2 \theta}{n_o^2} \sin^2 \alpha} \right) \\ &+ \frac{2\pi d_3}{\lambda} \left(\sqrt{n_{os}^2 - \sin^2 \alpha} - \sqrt{n_{es}^2 - \frac{n_{es}^2 \sin^2 \theta + n_{os}^2 \cos^2 \theta}{n_{os}^2} \sin^2 \alpha} \right) \\ &+ \frac{2\pi d_4}{\lambda} \left(\sqrt{n_{es}^2 - \frac{n_{es}^2 \cos^2 \theta + n_{os}^2 \sin^2 \theta}{n_{os}^2} \sin^2 \alpha} - \sqrt{n_{os}^2 - \sin^2 \alpha} \right), \end{aligned} \quad (6)$$

where the refractive indices of the quartz and sapphire crystals at 632.8 nm are $n_e=1.552$, $n_o=1.543$ and $n_{es}=1.758$, $n_{os}=1.766$, respectively, while the incident angle $\alpha=\pm 20^\circ$ and the azimuthal angle of the incident planes $\theta\in[0^\circ, 360^\circ]$.

Table 2 Design and production values of plate thickness and phase retardation of the 632.8nm WVA $\lambda/4$ plate

Thickness of four crystal pieces		Phase retardation	
Design value	Production value	Design value	Theoretical value
$d_1=584.2 \mu\text{ m}$	$d_1=592.0 \mu\text{ m}$	$90^\circ\pm 0.5^\circ$	$90^\circ\pm 4.0^\circ$
$d_2=566.6 \mu\text{ m}$	$d_2=576.4 \mu\text{ m}$		
$d_3=848.4 \mu\text{ m}$	$d_3=836.8 \mu\text{ m}$		
$d_4=848.4 \mu\text{ m}$	$d_4=834.6 \mu\text{ m}$		

The thicknesses of all four crystal pieces in the 632.8nm WVA $\lambda/4$ plate were measured using the Optisurf system from Trioptics (Figure 5). The measured results from the second column of Table 2 were substituted into (6), to give a value for the phase retardation of $90^\circ\pm 4.0^\circ$, which is listed as the theoretical value in Table 2. To make the comparison between this theoretical value and the actual measurements clear, the correlations between the phase retardation and the incident angle of the WVA $\lambda/4$ plate were analysed for three selected states of the incident plane.



Fig.5. Optisurf thickness measurement system from Trioptics

The calculated and measured results for the phase retardation by the WVA $\lambda/4$ plate for the three selected states of the incident plane are illustrated in Figure 6. The theoretical values represent the trend of variation of the incident angle α calculated by substituting the actual thickness of the WVA $\lambda/4$ plate obtained with the Optisurf system into (6), for incident plane azimuthal angles θ of 0° , 45° , and 90° .

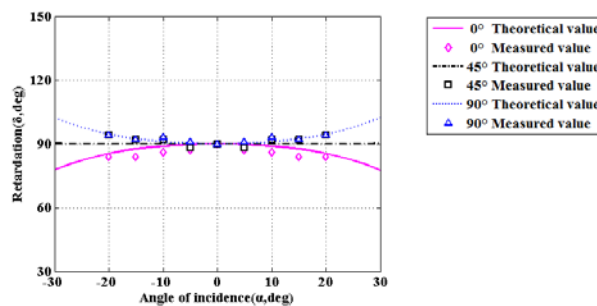


Fig.6. Theoretical and measured values of the phase retardation by a WVA $\lambda/4$ plate

The measured values demonstrate that the phase retardation by the target waveplate can be confined to a zone of $90^\circ\pm 6^\circ$ for incident angles in the range between $\pm 20^\circ$: the measured retardation is observed to vary between 84° and 96° as the incident angle turns from -20° to $+20^\circ$,

giving a margin of error of less than $\pm 6^\circ$. As an example, the difference between the measured and theoretical values of the retardation is approximately 2° for an incident plane azimuthal angle $\theta=0^\circ$.

It can also be seen from Figure 6 that for an incident plane of azimuthal angle $\theta=45^\circ$, the measured curve differs from the theoretical calculation, although in theory the incident angle should not affect the phase retardation. There are four main factors that can account for this phenomenon. First, the difference could be caused by uncertainties in the refractive indices of the quartz and sapphire crystals at the wavelength of 632.8nm. Second, manufacturing deviations exist in the optical axis of the WVA $\lambda/4$ plate, despite the elimination of such deviations in the plate thickness. Although additional retardation caused by thickness deviations can be removed by using the actually measured waveplate thickness when computing the theoretical values, uncertainty in the phase retardation measurements can also be caused by manufacturing deviations in the optical axis of the waveplate. Third, errors in the installation and adjustment of the WVA $\lambda/4$ plate can also generate changes in phase retardation. Fourth, the precision of the group of devices shown in Figure 2 is limited to 2° .

CONCLUSION

The angles of incidence at the mask level can vary up to $\pm 20^\circ$ in a high-NA (1.35) lithographer. To determine the cancelling effects of a WVA $\lambda/4$ plate on the phase retardation by a conventional $\lambda/4$ plate caused by a ray obliquely incident at between $\pm 20^\circ$, a 632.8 nm WVA $\lambda/4$ plate composed of two pieces of negative sapphire crystal and two pieces of positive quartz crystal were designed and manufactured. Experiments showed that the phase retardation by the WVA $\lambda/4$ plate was consistently in the range between 84° and 96° for incident angles between $\pm 20^\circ$, which demonstrated the effectiveness of the combination of quartz and sapphire in eliminating the influence of oblique incidence on phase retardation. The principles and experimental design described in this paper can thus be applied to verification of the phase retardation characteristics of a WVA $\lambda/4$ plate.

ACKNOWLEDGMENTS

The authors gratefully acknowledge the help of members of the Key Laboratory of Photoelectron Imaging Technology and Systems with the experiments described in this paper. This work was supported by the National Basic Research Program of China (973 Program) (No. 2012CB719705) and the National Key Technology Support Program of China (No.2015BAK10B02).

REFERENCES

- [1] Y. Qiongyan and W. Xiangzhao: 'Recent development of international mainstream lithographic tools', *Laser & Optoelectronics Progress*, 2007,44(1):57-64.
- [2] Gong Yan and Zhangwei: 'Present status and progress in 193nm exposure system in lithography', *Chinese Journal of Optics and Applied Optics*, 2008,1(1): 25-35.
- [3] Sun Yingzi, Wang Dongguang et.al: 'On the intensity method for measuring waveplate phase decay', *Astronomical Research and Technology*, 2008,5(1):74-82.
- [4] Bo Feng, Zhu Jianqiang and Kang Jun: 'Precise measurement and factors analysis for phase retardation of wave plate', *Chinese Journal of Lasers*, 2007,34(6):851-856.
- [5] Cao Guorong, Pan Bo and Wang Zhenglinig: 'Measuring of phase retardation and calibration of fast axis of wave plates', *Laser Journal*, 2012,33(4):20-21.
- [6] Wang Baoxi: 'Measurement Method and Technology for Phase Retardation of Light'. Dissertation. ShanDong: Qufu Normal University, 2012.
- [7] Zhang Jingbin and Li Guohua: 'Feasible study on the measurement of phase delay of mica plate by interference method', *Optoelectronics Laser*, 1997,8(3):202-204.
- [8] Jin Guopan and Li Jingzhen: *Laser Metrology*. Beijing: Science Press, 1998.
- [9] Fan Ling and Song Feijun: 'Spectrum analysis of modulated polarized light in phase retardation

- measurement', *Spectroscopy and Spectral Analysis*, 2007,27(9):1685-1688.
- [10] Liang Quanting: *Physical Optics*. Beijing: China Machine Press, 1980.
- [11] Lin Yao, Zhou Zhiyao and Wang Renwang: 'Optical heterodyne measurement of phase retardation of wave plate', *Acta Optica Sinica*, 1987,7(10):929-934.
- [12] Zuo Fen, Chen Lei and Xu Chen: 'Dynamic phase-shifting interferometry for full field retardation distribution of quarter wave plate', *Acta Photonica Sinica*, 2008,37(11):2296-2299.
- [13] Yan Ming and Gao zhishan: 'Phase shifting method for measuring the phase retardation of wave plates', *Journal of Optoelectronics Laser*, 2005,16(2):183-187.
- [14] Yan Ming and Gao Zhisan: 'The simple method research for measuring the phase retardation of wave plates', 2005,*Laser Technology*, 29(3):233-236.
- [15] Fan Shuhai, Song Lianke, Peng Handong and Zhang Dongqing: 'Two-dimensional measurement for optical phase retardation', *Laser Journal*, 2003,24(1):12-14.
- [16] Zhang Xu, Wu Fuquan, Wang Hailong and Hao Dianzhong: 'Application of Nd₂Fe₁₄B in high temperature superconducting magnetic suspension technology experiment', *Physics Experimentation*, 2007,27(3):42-45.
- [17] Zhao Tingsheng, Li Guohua, Peng Handong and Zhou Wenping: 'Phase shift measurement of a retarder based on Fourier analysis', *Acta Optica Sinica*, 2008,28(1):105-109.
- [18] Juan Dong and Yanqiu Li: 'Analysis and optimization approaches for wide-viewing-angle $\lambda/4$ plate in polarimetry for immersion lithography', *JVSTB*, 2013, 31(1):011602-1-011602-7.